


Ultrafast control of spin-orbital separation probed with time-resolved resonant inelastic x-ray scattering

Aaron Müller[✉], Francesco Grandi[✉], and Martin Eckstein

Department of Physics, University of Erlangen-Nürnberg, 91058 Erlangen, Germany

 (Received 25 November 2021; revised 12 July 2022; accepted 2 September 2022; published 15 September 2022)

Quasi-one-dimensional systems exhibit many-body effects elusive in higher dimensions. A prime example is spin-orbital separation, which has been measured by resonant inelastic x-ray scattering (RIXS) in Sr_2CuO_3 . Here, we theoretically analyze the time-resolved RIXS spectrum of Sr_2CuO_3 under the action of a time-dependent electric field. We show that the external field can reversibly modify the parameters in the effective t - J model used to describe spinon and orbiton dynamics in the material. For strong driving amplitudes, we find that the spectrum changes qualitatively as a result of reversing the relative spinon to orbiton velocity. The analysis shows that in general, the spin-orbital dynamics in Mott insulators in combination with time-resolved RIXS should provide a suitable platform to explore the reversible control of many-body physics in the solid with strong laser fields.

DOI: [10.1103/PhysRevB.106.L121107](https://doi.org/10.1103/PhysRevB.106.L121107)

Introduction. Electrons in strongly correlated materials can be characterized by charge, spin, and orbital quantum numbers. In a prototypical Mott insulator, the charge becomes localized by the electron-electron repulsion, leading to highly intertwined spin-orbital physics and a variety of ordering phenomena [1]. In low-dimensional materials, the effect of the Coulomb repulsion can be even more exotic, and the electron can fractionalize into spin and orbital excitations [spin-orbital separation (SOS)] [2,3] in analogy to spin-charge separation (SCS) [4–6]. Ultrashort laser pulses have opened avenues to control the many-particle physics in solids out of equilibrium [7–9]. A particularly versatile concept is Floquet engineering, where the Hamiltonian of a system is dynamically modified with time-periodic fields, as employed widely in optical lattice experiments [10–13]. For example, a control of SCS has been proposed through Floquet engineering of the t - J model [14]. In solids, however, a major challenge to implement a similar dynamic control is the heating due to photon absorption from the drive. Few theoretical proposals have so far been realized, such as Floquet-Bloch states of weakly interacting electrons [15–17]. Only very recently, a seminal experiment has shown the Floquet control of nonlinear local properties in a strongly correlated compound [18].

In this Letter, we show that the spin and orbital degrees of freedom in Mott insulators provide a promising platform to realize a dynamic control of dispersive many-body physics in solids, and in particular, electron fractionalization. As discussed in Ref. [18], the Mott gap implies a large transparency window that limits heating via multiphoton absorption, as needed for Floquet engineering. A large gap can also make the insulator robust against tunneling breakdown in static fields [19,20]. This allows for alternative, less explored pathways to control the low-energy spin-orbital physics with slowly varying strong field transients. Moreover, spin-orbital excitations can be probed using resonant inelastic x-ray scattering (RIXS)

[21,22], and recent upgrades of free-electron lasers should provide a sufficient time (~ 30 fs) and energy (~ 0.05 eV) resolution to resolve their dynamics [23,24].

We particularly focus on the charge-transfer insulator Sr_2CuO_3 . The spin-orbital excitations in this material are well described by an effective t - J model, where t refers to the hopping matrix element for an orbital excitation, which is very different from the original electronic tunneling, and J is the usual spin exchange constant. The model displays signatures of SOS, as clearly visible in static RIXS [3]. The orbiton in Sr_2CuO_3 turns out to be slower than the spinon, with a speed comparable in magnitude ($J/t = 2.8$). Notice that this situation is very different from the typical case of SCS, where t refers to the original hopping of a charge excitation, which is typically much faster than the spinon. In the case of Sr_2CuO_3 , the ratio t/J should therefore be controllable over a wide range, eventually allowing for a nontrivial dynamic switch between distinct regimes in which the spinon is either faster or slower than the orbiton.

Equilibrium Hamiltonian. The quasi-one-dimensional charge-transfer insulator Sr_2CuO_3 can be described as a chain of alternating copper and oxygen atoms in $3d^9$ configuration and with filled $2p$ orbitals. This makes it convenient to work in a hole representation, with one hole per unit cell. The low point-group symmetry of the crystal entirely lifts the degeneracy of the Cu $3d$ orbitals, and the ground state is a Mott insulator with one hole in the $3d_{x^2-y^2}$ orbital (termed a in the following). Without any orbital excitation the Hamiltonian of the system is a Heisenberg model with antiferromagnetic exchange J . The motion of orbital excitations on top of this can be described by an effective t - J model [25], which is found well in agreement with experiment [3],

$$\mathcal{H}_{t-J} = -t \sum_{j,\sigma} (p_{j\sigma}^\dagger p_{j+1\sigma} + \text{H.c.}) - E \sum_j \tilde{n}_j + \mathcal{H}_s, \quad (1)$$

Here, the fermion operator $p_{j\sigma}$ creates an orbital excitation where a hole with spin σ at site j is transferred to another orbital b , and \tilde{n}_j counts the holes in the a orbital; S_j is the spin of the Cu hole, and $\mathcal{H}_s = J \sum_j (\mathcal{S}_j \mathcal{S}_{j+1} - \frac{1}{4} \tilde{n}_j \tilde{n}_{j+1})$ a Heisenberg Hamiltonian. An analogous Hamiltonian can be written for different orbitons. Here, we focus on $b \equiv 3d_{zx}$, which turns out to have the broadest dispersion among the $3d$ orbitals. To derive this model [25], the valence bands of Sr_2CuO_3 are described by an *ab initio* charge-transfer Hamiltonian \mathcal{H}_{c-t} with nearest-neighbor hopping, local Hubbard interaction and Hund's coupling, charge-transfer energy between the Cu and oxygen states, and a nearest-neighbor Coulomb repulsion [26] (for details, see the Supplemental Material [27]). The large electron-electron repulsion justifies a strong-coupling expansion, which projects out doubly occupied orbitals and Cu-O charge-transfer excitations, and results in a Kugel-Khomskii Hamiltonian [28] for the spin and orbital degrees of freedom of the Cu hole. Spin and orbital superexchange proceeds via the O $2p$ orbitals and is therefore obtained from a fourth-order perturbation expansion in the p - d hopping [29]. By neglecting spin-flip processes in the hopping of the hole in the b orbital, and choosing a Jordan-Wigner representation for the orbital pseudospin, the Kugel-Khomskii Hamiltonian is then mapped on the t - J model Eq. (1). In this way, $J > 0$ and t in Eq. (1) relate to the spin and orbital superexchange interaction, and E is related to the crystal field splitting. When the orbiton is present, the first part of Eq. (1) describes its motion in a Néel antiferromagnetic background. The equilibrium parameters in Eq. (1) for Sr_2CuO_3 are [25] $t \sim 0.085$ eV, $J \sim 0.238$ eV, and $E \sim 1.999$ eV. The large ratio $J/t \sim 2.8$ is indeed aberrant compared to the typical value of the spin-charge t - J model obtained from a single-band Hubbard model at large interaction U [30]. In the latter, the parameter t is the original electron hopping, and $J = 4t^2/U \ll t$, while in Eq. (1) both t and J originate from a fourth-order perturbation expansion.

Below we will analyze how external fields can be used to control t and J over a wide range, covering both $J/t > 2$ (fast spinon regime) and $J/t < 2$ (slow spinon regime).

To prepare for this analysis, we first discuss the equilibrium orbital spectral function $\chi(\omega, k) = -1/\pi \text{Im} G_k(\omega + i0^+)$ of the momentum-dependent single orbiton propagator G_k ; G_k is the Fourier transform $G_k = 1/L \sum_{j,j'=0}^{L-1} e^{ik(j'-j)} G_{j',j}$ of the real-space propagator

$$G_{j',j}(t', t) = -i \langle \Psi_0 | \mathcal{U}_s(t_0, t') p_{j'\sigma}^\dagger \mathcal{U}_{t-J}(t', t) p_{j\sigma} \mathcal{U}_s(t, t_0) | \Psi_0 \rangle. \quad (2)$$

Here, $|\Psi_0\rangle$ is the initial ground state (no orbital excitation) at time $t_0 \rightarrow -\infty$, and \mathcal{U}_s and \mathcal{U}_{t-J} denote the time evolution in the Heisenberg and t - J model, respectively. The resulting spectrum shows a distinct form in the slow [Fig. 1(a)] and fast [Fig. 1(b)] spinon regime. Note that the spectral function $\chi(\omega, k)$ of the effective t - J model corresponds to the dynamical momentum-dependent orbital structure factor of the electronic model. This quantity is entirely unrelated to the electronic spectral function, which measures final states at a different electron number [such as electron removal for an angle-resolved photoemission spectroscopy (ARPES) measurement [31]].

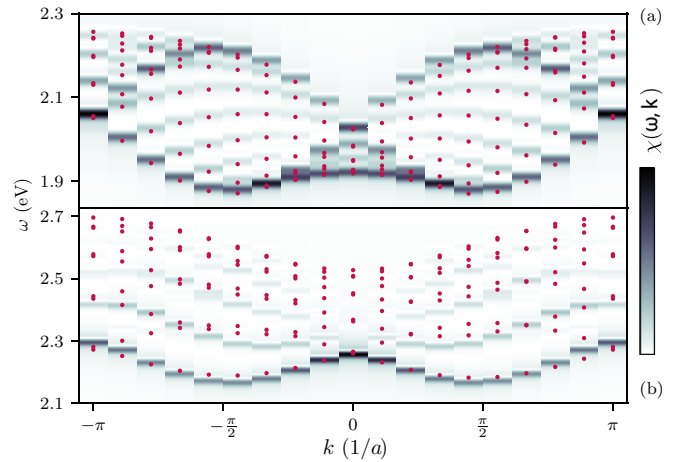


FIG. 1. Spectral function $\chi(\omega, k)$ in the (a) slow ($J/t = 0.4$) and (b) fast ($J/t = 2.8$) spinon regime, computed on a chain with $L = 18$ sites and Gaussian broadening. Red dots are obtained with the spin-orbital separation ansatz with $E_f = E + J$ and (a) $t_f = t$, $J_f = J$ and (b) $t_f = t/2$, $J_f = J$.

As a consequence of the spin-orbital separation, insight into the form of $\chi(\omega, k)$ can be acquired from a semiphenomenological spectral building principle [32,33]: Assuming that the orbital excitation separates into a spinon and an orbiton, which are treated as independent particles with dispersion $\epsilon_s(k_s) = \pi J_f/2 |\cos k_s|$ for $-\pi/2 \leq k_s \leq \pi/2$ [34] and $\epsilon_o(k_o) = E_f - 2t_f \cos k_o$, respectively, spectral weight in $\chi(\omega, k)$ should be found at energies $\epsilon(k) = \epsilon_s(k_s) + \epsilon_o(k_o)$, with a constraint $k = k_s + k_o$ due to momentum conservation. Hence, one expects the peaks of $\chi(\omega, k)$ at $\epsilon(k) = E_f - 2t_f \cos k_o + J_f \frac{\pi}{2} |\cos(k - k_o)|$. A $1/L$ correction to the momentum of the orbiton has to be applied on account of periodic boundary conditions [34,35]. In Fig. 1, $\epsilon(k)$ is shown by red dots. In the slow spinon regime, the spectrum is enclosed by the lower and upper orbiton branches [6,36], and there is an overall good agreement between the numerical results and $\epsilon(k)$. In the fast spinon regime, the spectral building principle still reproduces the lower bound of the spectrum, although the parameter t_f needs to be renormalized with respect to the bare t due to further dressing of the orbiton [37]. The transition between these two regimes can be located at the so-called supersymmetric point $J/t = 2$, where the t - J model becomes exactly solvable by the Bethe ansatz [38].

Nonequilibrium effective Hamiltonian. To include the effect of the driving laser, we couple the charge-transfer Hamiltonian \mathcal{H}_{c-t} to an electromagnetic field using the Peierls substitution [39,40]. In the length gauge within the electric-dipole approximation [41–43], this is equivalent to adding a scalar potential $\Phi_j(t) = -eE(t)X_j$ at each site (independent of the orbital), where e is the elementary charge, $E(t)$ the time-dependent electric field, and $X_j = j\tilde{a}/2$ represents the position along the chain, with the copper-copper distance $\tilde{a} \sim 0.392$ nm [44]. We neglect the renormalization of the hopping due to dipole matrix elements. Below, we parametrize the time dependence of the electric field as $E(t) = S(t) \cos(\Omega t)$, with an oscillatory part and an envelope $S(t)$ with maximum amplitude E_0 . The time-dependent modification of the parameters t and J is then understood in two distinct limits:

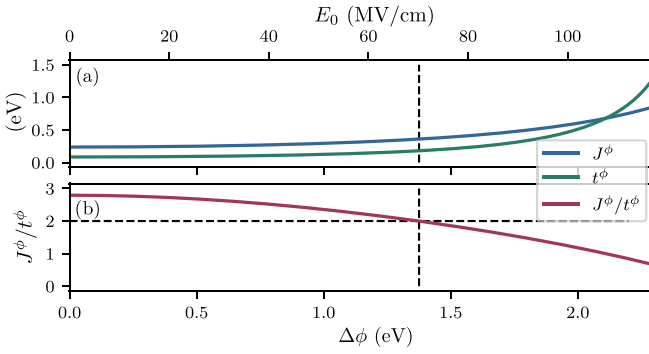


FIG. 2. (a) Effective parameters J^ϕ and t^ϕ vs the potential field gradient $\Delta\phi$ (electric field amplitude E_0) in the lower (upper) horizontal axis for the quasistatic regime and (b) the corresponding change in the characteristic value J/t . The horizontal dashed line shows the value $J/t = 2$ separating the slow and fast spinon regime.

In the quasistatic limit, one can derive a t - J Hamiltonian at a given time t by repeating the strong-coupling perturbation expansion including energy shifts of the orbitals caused by the instantaneous scalar potential difference $\Delta\phi = e\tilde{a}E(t)/2$ between neighboring sites. The potential modifies the virtual intermediate state of the perturbation expansion, and yields field-dependent parameters t^ϕ , J^ϕ , and E^ϕ in Eq. (1). (For explicit expressions, see the Supplemental Material [27].) This quasistatic argument should apply to slowly varying fields $\Omega \ll t, J$, up to several 10 THz given the values of t and J . Both J^ϕ and t^ϕ increase with $\Delta\phi$, leading to an overall decrease of the ratio J/t (Fig. 2). The intrinsic limitation to the quasistatic control of the spin-orbital physics is the tunneling breakdown of the insulating state, which would lead to a population of real charge-transfer excitations. The most rapid breakdown is expected when the gradient $\Delta\phi$ is resonant to the nearest-neighbor charge-transfer energy E_{CT} . Simulations in one- and two-band Hubbard models consistently show that the carrier generation rate becomes exponentially suppressed for fields sufficiently below E_{CT} [19,20,45]. The fields needed to decrease the ratio J/t below the supersymmetric point are well below this resonant amplitude $E_{CT} \sim 130$ MV/cm ($\Delta\phi_{CT} = 2.6$ eV) for the present system, so that a control of the spin-orbital physics should be possible at least transiently.

In the Floquet limit, one can conveniently write a time-periodic Hamiltonian in the Floquet basis by moving from the Fock space \mathcal{F} of the original problem to a larger space $\mathcal{F} \otimes \mathcal{T}$, with \mathcal{T} the Hilbert space of the square-integrable periodic functions with period $T = 2\pi/\Omega$. States in the extended space are labeled by an additional discrete index n , which can be understood as the number of photons absorbed or emitted relative to the drive. The representation of $\mathcal{H}(t)$ on the enlarged Fock space is called the Floquet Hamiltonian \mathcal{H}_{c-t}^{Fl} , which defines an effective static problem that describes the stroboscopic evolution of the driven system. Since \mathcal{H}_{c-t}^{Fl} is time independent, one can use a strong-coupling perturbation expansion analogous to the undriven case to derive the fourth-order spin-orbital superexchange interactions underlying the t - J model Eq. (1). The Floquet control of superexchange

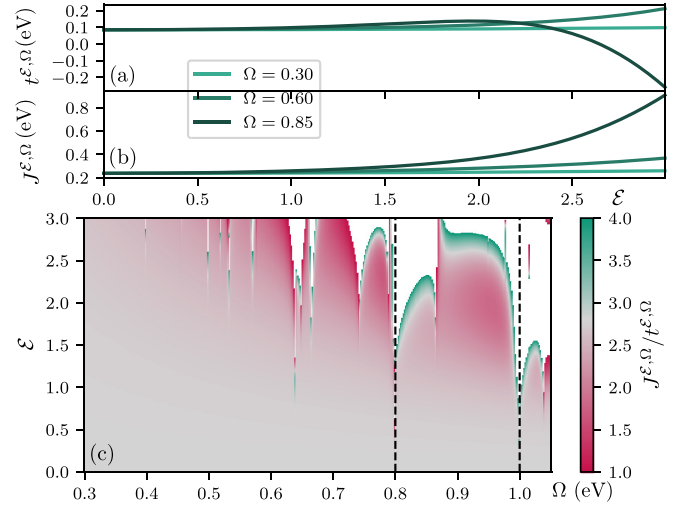


FIG. 3. [(a), (b)] Effective parameters $t^{\mathcal{E},\Omega}$ and $J^{\mathcal{E},\Omega}$ vs the Floquet parameter \mathcal{E} for several driving frequencies Ω . (c) $J^{\mathcal{E},\Omega}/t^{\mathcal{E},\Omega}$ as a function of Ω and \mathcal{E} . The white areas correspond to regimes in which $J^{\mathcal{E},\Omega}/t^{\mathcal{E},\Omega}$ lies outside the indicated range. The dashed lines show the leading Floquet resonances in the given frequency range, which involve a virtual transition to the $n = 4$ Floquet sector.

interactions has been derived for various situations, including exchange interactions in the magnetic [46–48] and charge sector [49] of the single-band Hubbard model, antisymmetric exchange interactions which may stabilize chiral spin liquids [50], and superexchange via ligand ions [51]. To derive the superexchange interaction in the Floquet representation in the present case, we project out both virtual charge excitations and states in Floquet sectors $n \neq 0$ (virtual photons). The emission or absorption of n virtual photons during an electronic hopping process shifts the energy of the intermediate states of the superexchange process by $\pm n\Omega$. The matrix elements for such processes are controlled by the Floquet parameter $\mathcal{E} = e\tilde{a}E_0/(2\Omega)$. Explicit calculations and results for the dependence of $t^{\mathcal{E},\Omega}$, $J^{\mathcal{E},\Omega}$, and $E^{\mathcal{E},\Omega}$ on \mathcal{E} and Ω are provided in the Supplemental Material [27].

In the following, Floquet theory is applied for frequencies $\Omega > t, J$, but below the optical gap $\Delta_{\text{gap}} \sim 1.6$ – 1.8 eV [52] to limit charge-transfer excitations due to linear photon absorption. By avoiding the Floquet resonances (resonant frequencies for which the intermediate-state energy in the superexchange process would vanish), one can further also limit multiphoton absorption. In contrast to what is observed in the quasistatic limit, it is possible to both decrease and increase the hopping $t^{\mathcal{E},\Omega}$ with respect to the equilibrium value [see Fig. 3(a)], while $J^{\mathcal{E},\Omega}$ can only increase in the analyzed domain [see Fig. 3(b)]. The ratio J/t can therefore be controlled in a wide range below the supersymmetric point $J/t = 2$ [see Fig. 3(c)]. For example, for $\Omega \sim 0.78$ eV the regime $J/t < 2$ is reached for a Floquet parameter $\mathcal{E} \sim 2$. Divergences of J/t appear upon increasing \mathcal{E} at fixed Ω due to a localization of the orbital ($t = 0$) when the spin excitations remain mobile [14].

Time-resolved RIXS. To verify the dynamic control over the superexchange interactions described in the previous section, one needs an experimental probe able to follow the transient change of the spectrum over the whole Brillouin

zone. Time-resolved RIXS (trRIXS) seems particularly suitable for this task. The incoming photon with energy ω_i , momentum k_i , and polarization e_i excites the hole originally in the a orbital to the $2p$ core state of a copper atom. This highly unstable intermediate state can decay within a few femtoseconds to the b orbital by emitting a photon with energy ω_f , momentum k_f , and polarization e_f , leaving the system with a d - d excitation. In principle, the hole can also decay into other d orbitals, but we are only interested in the b channel, as motivated previously. Thus, measuring the energy loss ($\omega = \omega_i - \omega_f$) and momentum loss ($k = k_i - k_f$) of the photon allows us to probe the excitation spectrum of the compound. For the short-lived intermediate state, one can apply the ultrashort core-hole approximation (UCA) [53], which describes the photon scattering via the intermediate state in terms of a single RIXS operator \mathcal{B} . The UCA is well established in interpreting static RIXS probes of the dynamics of spin and orbital excitations in equilibrium [3]. With core hole lifetimes in the range of few femtoseconds, the UCA remains justified also for trRIXS of processes on the 100 fs timescale, as in the present case. In the Supplemental Material [27], we derive the trRIXS signal within the UCA, starting from the general expression for trRIXS in terms of a four-point correlation function [54,55]. The result can be written as $I_{\text{RIXS}} = 2(|B_{e_i e_f}^{\uparrow\uparrow}|^2 + |B_{e_i e_f}^{\uparrow\downarrow}|^2)\chi(\omega, k, \bar{t})$. Here, $B_{e_i e_f}^{\uparrow\uparrow}$ and $B_{e_i e_f}^{\uparrow\downarrow}$ are the matrix elements of the RIXS operator [56,57], which will be the same for time-resolved and static RIXS, and $\chi(\omega, k, \bar{t})$ is the convolution of the propagator (2) with probe functions centered around a probe time \bar{t} , $\chi(\omega, k, \bar{t}) = i \int dt' dt s(t', \bar{t})s(t, \bar{t})e^{-i\omega(t-t')}G_k(t', t)$. The probe pulse is there described semiclassically by the Gaussian envelope $s(t, \bar{t}) = \exp[-(t - \bar{t})^2/(2\sigma_{\text{pr}}^2)]$.

In the following, instead of analyzing I_{RIXS} , we focus on $\chi(\omega, k, \bar{t})$, which does not depend on the details of the experimental apparatus used to measure the RIXS signal. Despite the similarity of the above relation for I_{RIXS} to the angle-resolved photoemission spectroscopy signal, the two quantities actually rely on different expressions for the effective hopping parameter t (see the Supplemental Material [27]). The numerical evaluation of the single hole propagator Eq. (2) is done using a Krylov time propagation scheme with middle point approximation for the time evolution [58–60].

Dynamic control. As elucidated in the previous sections, it is possible to achieve control over the parameters t and J of the effective t - J model Eq. (1) both in the quasistatic and the Floquet regime. Here, we explicitly demonstrate the time-dependent modification of the spectrum for the quasistatic limit. We choose the time-dependent profile $\Delta\phi(t)$ to be Gaussian with variance $\sigma_{\text{pu}} = 90$ fs and maximum value $\Delta\phi^{\text{max}} = 1.8$ eV, as depicted in Fig. 4(a).

In Figs. 4(b)–4(e), we show the time evolution of $\chi(\omega, k, \bar{t})$ during this time-dependent perturbation. At moderately strong values of the external field, the spectral function is not substantially changed with respect to equilibrium, even if quantitative differences can be observed [see Fig. 4(b)]. However, around the maximum $\Delta\phi^{\text{max}}$ one identifies a qualitative change in the spectrum, with the appearance of a well-defined upper orbital branch not present at lower values of the field [see Fig. 4(c)]. This is a signature of the transition from

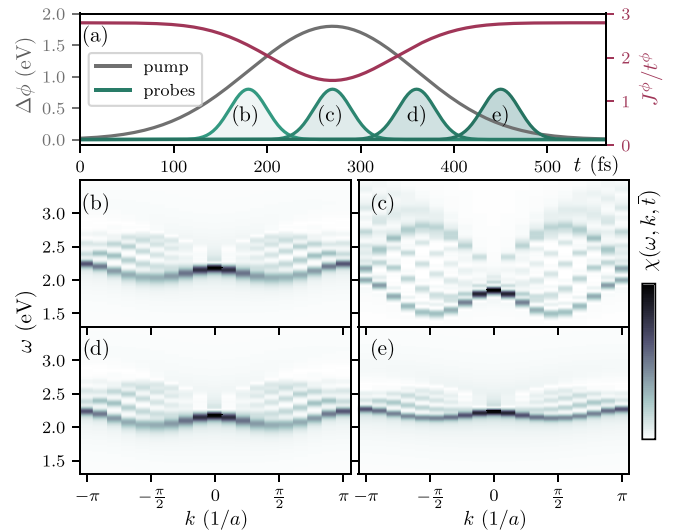


FIG. 4. (a) Time-dependent potential field gradient $\Delta\phi(t)$ ($\Delta\phi^{\text{max}} = 1.8$ eV, $\sigma_{\text{pu}} = 90$ fs) and resulting change in J/t . [(b)–(e)] Time-dependent evolution of the spectral function $\chi(\omega, k, \bar{t})$ for different probe envelopes with $\sigma_{\text{pr}} = 20$ fs and (b) $\bar{t} = 180$ fs, (c) $\bar{t} = 270$ fs, (d) $\bar{t} = 360$ fs, and (e) $\bar{t} = 450$ fs for a chain length $L = 18$.

the fast to the slow spinon regime. Indeed, as shown in Fig. 4(a), the values of the ratio J/t reached at $\Delta\phi^{\text{max}}$ are well below the supersymmetric point $J/t = 2$. As the pump strength decreases, the spectrum narrows into its equilibrium shape, which happens reversibly [see Figs. 4(d) and 4(e)]. This proves the possibility to dynamically control the qualitative shape of the spectral function and hence of the underlying collective excitations.

Conclusions. In conclusion, we showed that short pulses with realistic field amplitudes can be used to reversibly control the spin-orbital excitations in the quasi-one-dimensional compound Sr_2CuO_3 . These pulses can substantially change the relative strength of the t and J parameters in the effective t - J model which describes the spin and the orbital excitations in this material. This demonstrates control over the electronic fractionalization in solids between regimes where the spinon moves faster than the orbiton and the contrary one. More generally, the analysis illustrates that the spin-orbital physics in Mott insulators is a suitable platform to explore the reversible control of many-body dynamics in solids with strong laser fields. In particular, with the improved energy resolution available at new generation free-electron lasers, spin-orbital excitations can be probed using trRIXS. Moreover, our analysis shows that a control of the low-energy physics can be achieved by two different pathways, i.e., Floquet engineering and a subcycle control with strong THz transients, which can be seen as two limits of a more general control of exchange interactions with arbitrary time-dependent fields [61]. The spatially anisotropic character of the orbital-orbital interaction, as opposed to the isotropic spin-spin one, suggests a different physics in the two situations. Indeed, the light modulation of the orbital exchange interaction leads to a switch of the state of the system from a discrete minimum to another, each corresponding to distinguishable orbital orders [62]. Besides the exemplary compound (Sr_2CuO_3) we

considered, further Mott systems show spin-orbital separation, and we expect a nontrivial dynamic control in CaCu_2O_3 [63] or Ca_2CuO_3 [64], the light control of multispinon excitations in Sr_2CuO_3 [65], and the control of two-spinon and two-orbital excitations in the spin-Peierls compound TiOCl [66].

Acknowledgments. We thank Matteo Mitrano for useful discussions. This work was supported by the ERC Starting Grant No. 716648. The authors gratefully acknowledge the computational resources and support provided by the Regional Computing Center Erlangen (RRZE).

-
- [1] Y. Tokura and N. Nagaosa, Orbital physics in transition-metal oxides, *Science* **288**, 462 (2000).
- [2] K. Wohlfeld, M. Daghofer, S. Nishimoto, G. Khaliullin, and J. van den Brink, Intrinsic Coupling of Orbital Excitations to Spin Fluctuations in Mott Insulators, *Phys. Rev. Lett.* **107**, 147201 (2011).
- [3] J. Schlappa, K. Wohlfeld, K. J. Zhou, M. Mourigal, M. W. Haverkort, V. N. Strocov, L. Hozoi, C. Monney, S. Nishimoto, S. Singh, A. Revcolevschi, J.-S. Caux, L. Patthey, H. M. Ronnow, J. van den Brink, and T. Schmitt, Spin-orbital separation in the quasi-one-dimensional Mott insulator Sr_2CuO_3 , *Nature (London)* **485**, 82 (2012).
- [4] E. H. Lieb and F. Y. Wu, Absence of Mott Transition in an Exact Solution of the Short-Range, One-Band Model in One Dimension, *Phys. Rev. Lett.* **20**, 1445 (1968).
- [5] C. Kim, A. Y. Matsuura, Z.-X. Shen, N. Motoyama, H. Eisaki, S. Uchida, T. Tohyama, and S. Maekawa, Observation of Spin-Charge Separation in One-Dimensional SrCuO_2 , *Phys. Rev. Lett.* **77**, 4054 (1996).
- [6] B. J. Kim, H. Koh, E. Rotenberg, S.-J. Oh, H. Eisaki, N. Motoyama, S. Uchida, T. Tohyama, S. Maekawa, Z.-X. Shen, and C. Kim, Distinct spinon and holon dispersions in photoemission spectral functions from one-dimensional SrCuO_2 , *Nat. Phys.* **2**, 397 (2006).
- [7] C. Giannetti, M. Capone, D. Fausti, M. Fabrizio, F. Parmigiani, and D. Mihailovic, Ultrafast optical spectroscopy of strongly correlated materials and high-temperature superconductors: A non-equilibrium approach, *Adv. Phys.* **65**, 58 (2016).
- [8] D. N. Basov, R. D. Averitt, and D. Hsieh, Towards properties on demand in quantum materials, *Nat. Mater.* **16**, 1077 (2017).
- [9] A. de la Torre, D. M. Kennes, M. Claassen, S. Gerber, J. W. McIver, and M. A. Sentef, Colloquium: Nonthermal pathways to ultrafast control in quantum materials, *Rev. Mod. Phys.* **93**, 041002 (2021).
- [10] G. Jotzu, M. Messer, R. Desbuquois, M. Lebrat, T. Uehlinger, D. Greif, and T. Esslinger, Experimental realization of the topological Haldane model with ultracold fermions, *Nature (London)* **515**, 237 (2014).
- [11] F. Görg, K. Sandholzer, J. Minguzzi, R. Desbuquois, M. Messer, and T. Esslinger, Realization of density-dependent Peierls phases to engineer quantized gauge fields coupled to ultracold matter, *Nat. Phys.* **15**, 1161 (2019).
- [12] J. Struck, C. Ölschläger, M. Weinberg, P. Hauke, J. Simonet, A. Eckardt, M. Lewenstein, K. Sengstock, and P. Windpassinger, Tunable Gauge Potential for Neutral and Spinless Particles in Driven Optical Lattices, *Phys. Rev. Lett.* **108**, 225304 (2012).
- [13] F. Görg, M. Messer, K. Sandholzer, G. Jotzu, R. Desbuquois, and T. Esslinger, Enhancement and sign change of magnetic correlations in a driven quantum many-body system, *Nature (London)* **553**, 481 (2018).
- [14] H. Gao, J. R. Coulthard, D. Jaksch, and J. Mur-Petit, Anomalous Spin-Charge Separation in a Driven Hubbard System, *Phys. Rev. Lett.* **125**, 195301 (2020).
- [15] T. Oka and H. Aoki, Photovoltaic Hall effect in graphene, *Phys. Rev. B* **79**, 081406(R) (2009).
- [16] Y. H. Wang, H. Steinberg, P. Jarillo-Herrero, and N. Gedik, Observation of Floquet-Bloch states on the surface of a topological insulator, *Science* **342**, 453 (2013).
- [17] J. W. McIver, B. Schulte, F.-U. Stein, T. Matsuyama, G. Jotzu, G. Meier, and A. Cavalleri, Light-induced anomalous Hall effect in graphene, *Nat. Phys.* **16**, 38 (2020).
- [18] J.-Y. Shan, M. Ye, H. Chu, S. Lee, J.-G. Park, L. Balents, and D. Hsieh, Giant modulation of optical nonlinearity by Floquet engineering, *Nature (London)* **600**, 235 (2021).
- [19] T. Oka and H. Aoki, Dielectric breakdown in a Mott insulator: Many-body Schwinger-Landau-Zener mechanism studied with a generalized Bethe ansatz, *Phys. Rev. B* **81**, 033103 (2010).
- [20] M. Eckstein, T. Oka, and P. Werner, Dielectric Breakdown of Mott Insulators in Dynamical Mean-Field Theory, *Phys. Rev. Lett.* **105**, 146404 (2010).
- [21] L. J. P. Ament, M. van Veenendaal, T. P. Devereaux, J. P. Hill, and J. van den Brink, Resonant inelastic x-ray scattering studies of elementary excitations, *Rev. Mod. Phys.* **83**, 705 (2011).
- [22] M. Mitrano and Y. Wang, Probing light-driven quantum materials with ultrafast resonant inelastic x-ray scattering, *Commun. Phys.* **3**, 184 (2020).
- [23] M. Dunne, LCLS strategic facility development plan, https://lcls.slac.stanford.edu/sites/default/files/LCLS_Strategic_Development_Plan.pdf (2020).
- [24] M. Dunne, X-ray free-electron lasers light up materials science, *Nat. Rev. Mater.* **3**, 290 (2018).
- [25] K. Wohlfeld, S. Nishimoto, M. W. Haverkort, and J. van den Brink, Microscopic origin of spin-orbital separation in Sr_2CuO_3 , *Phys. Rev. B* **88**, 195138 (2013).
- [26] R. Neudert, S.-L. Drechsler, J. Málek, H. Rosner, M. Kielwein, Z. Hu, M. Knupfer, M. S. Golden, J. Fink, N. Nücker, M. Merz, S. Schuppler, N. Motoyama, H. Eisaki, S. Uchida, M. Domke, and G. Kaindl, Four-band extended Hubbard Hamiltonian for the one-dimensional cuprate Sr_2CuO_3 : Distribution of oxygen holes and its relation to strong intersite Coulomb interaction, *Phys. Rev. B* **62**, 10752 (2000).
- [27] See Supplemental Material at <http://link.aps.org/supplemental/10.1103/PhysRevB.106.L121107> for a detailed derivation of the effective t - J model in the presence or in the absence of an electric field (in the quasistatic and Floquet limits) starting

- from an *ab-initio* charge transfer Hamiltonian, for a derivation of the time-dependent ultrashort core-hole approximation and for a comparison between the *t*-*J* models to describe RIXS and ARPES.
- [28] K. I. Kugel and D. I. Khomskii, The Jahn-Teller effect and magnetism: transition metal compounds, *Sov. Phys. Usp.* **25**, 231 (1982).
- [29] J. Zaanen and A. M. Oleś, Canonical perturbation theory and the two-band model for high- T_c superconductors, *Phys. Rev. B* **37**, 9423 (1988).
- [30] K. A. Chao, J. Spalek, and A. M. Oles, Kinetic exchange interaction in a narrow S-band, *J. Phys. C* **10**, L271 (1977).
- [31] Y. Wang, M. Claassen, C. D. Pemmaraju, C. Jia, B. Moritz, and T. P. Devereaux, Theoretical understanding of photon spectroscopies in correlated materials in and out of equilibrium, *Nat. Rev. Mater.* **3**, 312 (2018).
- [32] R. Eder and Y. Ohta, Photoemission spectra of the *t*-*J* model in one and two dimensions: Similarities and differences, *Phys. Rev. B* **56**, 2542 (1997).
- [33] R. N. Bannister and N. d'Ambrumenil, Spectral functions of half-filled one-dimensional Hubbard rings with varying boundary conditions, *Phys. Rev. B* **61**, 4651 (2000).
- [34] T. Giamarchi, *Quantum Physics in One Dimension*, illustrated ed., The International Series of Monographs on Physics Vol. 121 (Clarendon/Oxford University Press, Oxford, UK, 2004).
- [35] A. Bohrdt, D. Greif, E. Demler, M. Knap, and F. Grusdt, Angle-resolved photoemission spectroscopy with quantum gas microscopes, *Phys. Rev. B* **97**, 125117 (2018).
- [36] H. Suzuura and N. Nagaosa, Spin-charge separation in angle-resolved photoemission spectra, *Phys. Rev. B* **56**, 3548 (1997).
- [37] M. Brunner, F. F. Assaad, and A. Muramatsu, Single hole dynamics in the one-dimensional *t*-*J* model, *Eur. Phys. J. B* **16**, 209 (2000).
- [38] P.-A. Bares, G. Blatter, and M. Ogata, Exact solution of the *t*-*J* model in one dimension at $2t = \pm J$: Ground state and excitation spectrum, *Phys. Rev. B* **44**, 130 (1991).
- [39] R. Peierls, Zur Theorie des Diamagnetismus von Leitungselektronen. II Starke Magnetfelder, *Z. Phys.* **81**, 186 (1933).
- [40] J. Li, D. Golez, G. Mazza, A. J. Millis, A. Georges, and M. Eckstein, Electromagnetic coupling in tight-binding models for strongly correlated light and matter, *Phys. Rev. B* **101**, 205140 (2020).
- [41] H. R. Reiss, Effect of an intense electromagnetic field on a weakly bound system, *Phys. Rev. A* **22**, 1786 (1980).
- [42] T. B. Boykin, R. C. Bowen, and G. Klimeck, Electromagnetic coupling and gauge invariance in the empirical tight-binding method, *Phys. Rev. B* **63**, 245314 (2001).
- [43] D. Baykusheva and H. J. Wörner, *Attosecond molecular spectroscopy and dynamics*, Molecular Spectroscopy and Quantum Dynamics, edited by R. Marquardt and M. Quack (Elsevier, 2021), pp. 113–161, <https://www.sciencedirect.com/science/article/pii/B978012817234600009X>.
- [44] H. Rosner, H. Eschrig, R. Hayn, S.-L. Drechsler, and J. Málek, Electronic structure and magnetic properties of the linear chain cuprates Sr_2CuO_3 and Ca_2CuO_3 , *Phys. Rev. B* **56**, 3402 (1997).
- [45] N. Dasari, J. Li, P. Werner, and M. Eckstein, Revealing Hund's multiplets in Mott insulators under strong electric fields, *Phys. Rev. B* **101**, 161107(R) (2020).
- [46] J. H. Mentink, K. Balzer, and M. Eckstein, Ultrafast and reversible control of the exchange interaction in Mott insulators, *Nat. Commun.* **6**, 6708 (2015).
- [47] A. P. Itin and M. I. Katsnelson, Effective Hamiltonians for Rapidly Driven Many-Body Lattice Systems: Induced Exchange Interactions and Density-Dependent Hoppings, *Phys. Rev. Lett.* **115**, 075301 (2015).
- [48] M. Bukov, L. D'Alessio, and A. Polkovnikov, Universal high-frequency behavior of periodically driven systems: from dynamical stabilization to Floquet engineering, *Adv. Phys.* **64**, 139 (2015).
- [49] S. Kitamura and H. Aoki, η -pairing superfluid in periodically-driven fermionic Hubbard model with strong attraction, *Phys. Rev. B* **94**, 174503 (2016).
- [50] M. Claassen, H.-C. Jiang, B. Moritz, and T. P. Devereaux, Dynamical time-reversal symmetry breaking and photo-induced chiral spin liquids in frustrated Mott insulators, *Nat. Commun.* **8**, 1192 (2017).
- [51] S. Chaudhary, A. Ron, D. Hsieh, and G. Refael, Controlling ligand-mediated exchange interactions in periodically driven magnetic materials, [arXiv:2009.00813](https://arxiv.org/abs/2009.00813).
- [52] M. Imada, A. Fujimori, and Y. Tokura, Metal-insulator transitions, *Rev. Mod. Phys.* **70**, 1039 (1998).
- [53] Luuk J. P. Ament, F. Forte, and J. van den Brink, Ultrashort lifetime expansion for indirect resonant inelastic x-ray scattering, *Phys. Rev. B* **75**, 115118 (2007).
- [54] Y. Chen, Y. Wang, C. Jia, B. Moritz, A. M. Shvaika, J. K. Freericks, and T. P. Devereaux, Theory for time-resolved resonant inelastic x-ray scattering, *Phys. Rev. B* **99**, 104306 (2019).
- [55] M. Eckstein and P. Werner, Simulation of time-dependent resonant inelastic x-ray scattering using nonequilibrium dynamical mean-field theory, *Phys. Rev. B* **103**, 115136 (2021).
- [56] P. Marra, K. Wohlfeld, and J. van den Brink, Unraveling Orbital Correlations with Magnetic Resonant Inelastic X-Ray Scattering, *Phys. Rev. Lett.* **109**, 117401 (2012).
- [57] P. Marra, Theoretical approach to direct resonant inelastic x-ray scattering on magnets and superconductors, [arXiv:1605.03189](https://arxiv.org/abs/1605.03189).
- [58] S. R. Manmana, A. Muramatsu, and R. M. Noack, Time evolution of one-dimensional quantum many body systems, in *Lectures on the Physics of Highly Correlated Electron Systems IX: Ninth Training Course in the Physics of Correlated Electron Systems and High- T_c Superconductors*, edited by A. Avella and F. Mancini, AIP Conf. Proc. Vol. 789 (AIP, Melville, NY, 2005), p. 269, doi: [10.1063/1.2080353](https://doi.org/10.1063/1.2080353).
- [59] A. Alvermann, H. Fehske, and P. B. Littlewood, Numerical time propagation of quantum systems in radiation fields, *New J. Phys.* **14**, 105008 (2012).
- [60] P. Weinberg and M. Bukov, QuSpin: A Python package for dynamics and exact diagonalisation of quantum many body systems. Part II: Bosons, fermions and higher spins, *SciPost Phys.* **7**, 020 (2019).
- [61] M. Eckstein, J. H. Mentink, and P. Werner, Designing spin and orbital exchange Hamiltonians with ultrashort electric field transients, [arXiv:1703.03269](https://arxiv.org/abs/1703.03269).
- [62] F. Grandi and M. Eckstein, Fluctuation control of nonthermal orbital order, *Phys. Rev. B* **103**, 245117 (2021).
- [63] V. Bisogni, K. Wohlfeld, S. Nishimoto, C. Monney, J. Trinckauf, K. Zhou, R. Kraus, K. Koepf, C. Sekar, V.

- Strocov, B. Büchner, T. Schmitt, J. van den Brink, and J. Geck, Orbital Control of Effective Dimensionality: From Spin-Orbital Fractionalization to Confinement in the Anisotropic Ladder System CaCu_2O_3 , *Phys. Rev. Lett.* **114**, 096402 (2015).
- [64] R. Fumagalli, J. Heverhagen, D. Betto, R. Arpaia, M. Rossi, D. Di Castro, N. B. Brookes, M. Moretti Sala, M. Daghofer, L. Braicovich, K. Wohlfeld, and G. Ghiringhelli, Mobile orbitons in Ca_2CuO_3 : Crucial role of Hund's exchange, *Phys. Rev. B* **101**, 205117 (2020).
- [65] J. Schlappa, U. Kumar, K. J. Zhou, S. Singh, M. Mourigal, V. N. Strocov, A. Revcolevschi, L. Patthey, H. M. Ronnow, S. Johnston, and T. Schmitt, Probing multi-spinon excitations outside of the two-spinon continuum in the antiferromagnetic spin chain cuprate Sr_2CuO_3 , *Nat. Commun.* **9**, 5394 (2018).
- [66] S. Glawion, J. Heidler, M. W. Haverkort, L. C. Duda, T. Schmitt, V. N. Strocov, C. Monney, K. J. Zhou, A. Ruff, M. Sing, and R. Claessen, Two-Spinon and Orbital Excitations of the Spin-Peierls System TiOCl , *Phys. Rev. Lett.* **107**, 107402 (2011).